JOURNAL OF SPACECRAFT AND ROCKETS
Vol. 42, No. 6, November–December 2005

Hypersonic Shear Layer Stability Experiments

Anatolii A. Maslov,* Sergei G. Mironov,† and Vladimir M. Aniskin‡
Russian Academy of Sciences, 630090, Novosibirsk, Russia

Results from the study of hypersonic shear layer stability at high Mach number ($M_\infty = 21$) and moderate unit Reynolds number are reported, including electron-beam data for natural perturbations in the shock layer on a 7-deg sharp cone and data on the stability of laminar hypersonic near-wake flows against natural and artificial disturbances.

Nomenclature

C_x	=	dimensionless longitudinal phase velocity, $(2\pi \cdot f \cdot \Delta x)/(\Delta\varphi_x \cdot U_e)$
C_ϕ	=	dimensionless azimuthal phase velocity, $(2\pi \cdot f \cdot \Delta l)/(\Delta\varphi_l \cdot U_e)$
d_c	=	cone base diameter, m
d_w	=	outer diameter of whistle, m
F	=	dimensionless frequency, $2\pi \cdot f/Re_{1e} \cdot U_e$
f	=	frequency, Hz
M	=	Mach number
M_∞	=	freestream Mach number
n	=	mean density (molecules concentration), m^{-3}
n_∞	=	freestream mean density, m^{-3}
n'	=	total density pulsations, m^{-3}
$n'(F)$	=	spectral density pulsations, m^{-3}
R	=	$\sqrt{Re_{xe}}$
Re_{xe}	=	local Reynolds number behind shock wave
$Re_{1\infty}$	=	freestream unit Reynolds number, m^{-1}
r_a	=	nozzle exit radii, m
T_w	=	model wall temperature, K
T_0	=	stagnation temperature, K
U_e	=	gas velocity behind shock wave, ms^{-1}
U_∞	=	freestream gas velocity, ms^{-1}
w'	=	power of density pulsations, arbitrary units
X	=	longitudinal (streamwise) coordinate
Y	=	normal to the stream axis coordinate
Z	=	coordinate along the electron beam
$-\alpha_i(F)$	=	increment of disturbances, $-\alpha_i(F) = 0.5 \cdot d(\ln[n'(F)])/dR$
Δl	=	distance between two points of measurement on arc of circle of wake, m
Δx	=	distance between two points of measurement in X direction, m
$\Delta\varphi_l$	=	difference of phase between two points on arc of circle, rad
$\Delta\varphi_x$	=	difference of phase between two points in X direction, rad
θ	=	angle of conical coordinate system, deg
ϕ	=	azimuthal angle in a plane parallel to the cone radius and perpendicular to the cone axis, rad
φ	=	phase, rad
χ	=	density wave inclination angle, $\chi = a\tan(C_x/C_\phi)$, deg

Subscripts

e	=	behind the shock wave
w	=	model wall
0	=	stagnation
∞	=	freestream

Received 1 February 2002; accepted for publication 10 September 2004.

*Professor and Deputy Director, Institute of Theoretical and Applied Mechanics, Siberian Branch; maslov@itam.nsc.ru. Member AIAA.

†Principal Researcher, Hypersonic Flow Laboratory, Institute of Theoretical and Applied Mechanics, Siberian Branch; mironov@itam.nsc.ru.

‡Researcher, Hypersonic Flow Laboratory, Institute of Theoretical and Applied Mechanics, Siberian Branch; aniskin@itam.nsc.ru.

Introduction

DEVELOPING space technology and high-speed planes have aroused considerable interest in the stability of hypersonic shear flows. The urgency of this research is related to the essential effect of the shear flow state (laminar or turbulent) upon the heat flux level, intensity of power, and vibration loads on the construction of hypersonic aircraft. Gaining data on the characteristics of initial boundary-layer perturbations is a problem of primary importance in studies of hypersonic flow stability. These characteristics largely determine the spectrum and amplification of perturbations in the downstream region of the boundary flow. The initial perturbations are generated in the region near the leading edge of the model. In this region, the local Reynolds numbers are still low, and the boundary flow represents a viscous shock layer. The urgency of the investigation of the disturbances in hypersonic wake flows is associated with the problem of aerodynamic interference in the hypersonic motion of many bodies, for example, in the course of multistage Earth-to-orbit vehicle separation. The state of the flow in the wake can directly affect the laminar–turbulent transition in the boundary layer of the apparatus moving in the wake behind the head body. To date the stability of shock layers and laminar hypersonic wake flows against natural and artificial disturbances has not been adequately studied.

Theoretical studies[1–8] predict that the instability characteristics of shear layers at high hypersonic Mach numbers differ substantially from those of moderately hypersonic flows. In the region of high hypersonic velocities ($M > 10$), there are only unit experimental researches on the disturbance characteristics in shear flows (in the boundary layer and wake). They were made as early as the sixties and seventies of the previous century. In the case of Mach number more than 16, probe methods and electron-beam methods were used to measure the total pulsations of the mass flow rate and temperature,[9] mass flow rate,[10] and density pulsations[11] in the boundary layer on the wall of a helium wind tunnel. The same methods were used to measure the total density pulsations and density pulsation spectra in a mixing layer in the working section of the nitrogen wind tunnel with a freejet.[12,13] These data, however, can hardly be compared to each other, or to the calculations, because they are affected by the whole prehistory of the gas flow in the stagnation chamber and in the nozzle of a certain wind tunnel. Among rather new investigations is a paper by Lisenko,[14] in which the stability of a viscous shock layer on the plate was studied by a hot-wire anemometer method for $M_\infty = 21$ and moderate unit Reynolds numbers. Unfortunately, when the hot-wire anemometer is used in high-enthalpy flows of low

density, there are many problems in interpreting the data of these measurements.[15] Published research on hypersonic flow around a model for Mach numbers of $M = 19$–25 and moderate Reynolds numbers[16–19] describes the data obtained merely for the average stream parameters in the shock layer and on the surface. Only one paper[20] is known in which at $M = 8.5$–10.5 the position of the transition point was found on the cone, and the velocity of the disturbance motion was measured. A similar situation is reported for investigation in the hypersonic wake. In Refs. 21–23 the only data on the mean parameters and the position of the laminar–turbulent transition point in the wake are presented for Mach numbers less than 16.

Comprehensive data on the wave characteristics of the disturbances are needed to check the existing models of the developing instabilities in the shear flows and to develop new models. These data can be obtained only by local measurements, similar to those ones used in subsonic and supersonic streams. The present paper reports some experimental data that clarify in part some of the questions posed in this introduction.

Instrumentation, Models, and Measurement Technique

Wind Tunnel

The experiments were carried out in the T-327 open-type free-jet nitrogen hypersonic wind tunnel of the Institute of Theoretical and Applied Mechanics, Siberian Branch, Russian Academy of Sciences, at a freestream Mach number M_∞ of 21 and unit Reynolds number $Re_{1\infty} = 6 \times 10^5$ m^{-1}. The flow velocity in the test section of the wind tunnel is $U_\infty \cong 1500$ m/s, the run time is about 200 s, the stagnation temperature $T_0 = 1200$ K, and the streamwise uniformity of the Mach number is 3 units per meter. The nozzle exit diameter is 0.22 m and the uniform core of the flow is 0.1 m in diameter. The stagnation pressure in the experiments was maintained constant within 1%, and the stagnation temperature during the wind tunnel's run time varied less than ± 50 K.

According to electron-beam[24] and acoustic probe data, the level of total density pulsations along the streamwise axis at the test conditions is about 0.5% of the mean density; this level increases toward the periphery of the core flow (Fig. 1a). It is seen that predominant occurrence of inclined density waves is a specific feature of disturbances in the freestream. Figure 1b shows the normalized spectrum of freestream density pulsations and the normalized spectrum of inclination angles of density waves. The data were obtained by the method of electron-beam fluorescence.[24] Such flow perturbations, generated in the range of moderate Mach numbers and high Reynolds numbers, are most likely caused by boundary-layer instabilities that develop on the nozzle wall near the critical section of the nozzle.

Cone Models

Characteristics of flow disturbances in the shock layer of a cone are measured on a sharp cone model with a 7-deg half-angle. The model was made from aluminum with a carbon-black surface; this allowed us to minimize the parasitic effects caused by the emission of secondary electrons and light reflection. The length of the cone is 0.205 m, and its base diameter d_c is 0.04 m. The bluntness radius of the nose of the cone is no greater than 0.05 mm. The surface of the model is randomly grainy; the typical height of the surface roughness is about 10–20 μm. The model wall temperature was measured by a copper–constantan thermocouple situated at half-length of the cone generator. The model is not thermally stabilized and during the run time of the wind tunnel the temperature factor T_w/T_o of its surface varies linearly from 0.24 to 0.28. The cone is mounted on a wedge-shaped strut (base width 5 mm, wedge angle 10 deg) and fixed to it with the help of a 0.1-mm-long rod, 5 mm in diameter, that is mounted at the center of the cone base.

Characteristics of natural disturbances in the laminar near-wake flow are measured in the wake of the sharp cone. In this case, the cone half-angle is 10 deg, the cone length is 0.113 m, and the base diameter d_c is 0.04 m. The cone is mounted directly from its base to a wedge-shaped strut, the base thickness of which is 5 mm and wedge angle is 10 deg. The cone bluntness, the surface-relief characteristics, and the variations of the surface temperature factor are the same as in the experiments with the shock layer on the 7-deg sharp cone.

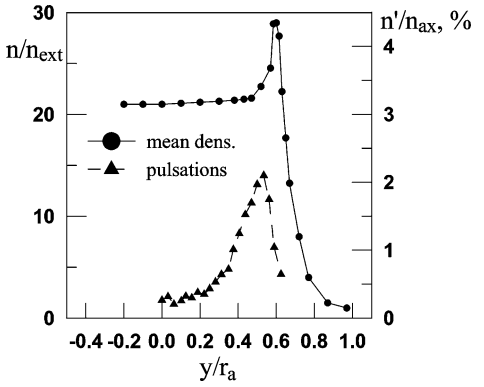

Fig. 1a Distribution of the mean density n/n_{ext} and the normalized total density pulsations n'/n_{ax} across the nozzle exit plane under the adopted experimental conditions. n_{ext} is the gas density outside the jet flow and n_{ax} is the mean density at the stream axis.

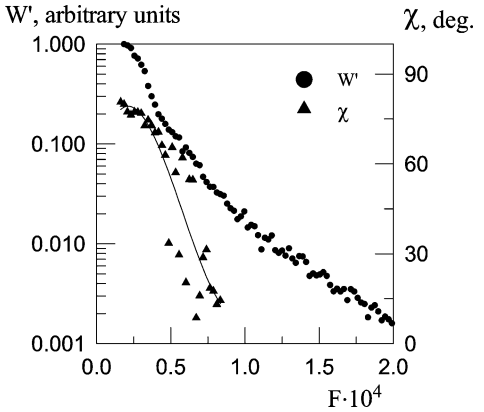

Fig. 1b Spectrum of power of density pulsations w' in the freestream and spectrum of inclination angles χ of density waves.

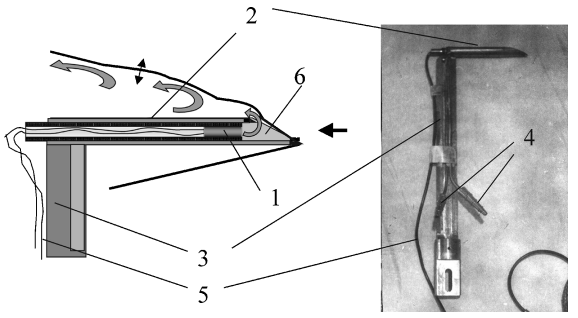

Fig. 2 Scheme and photo of the oblique-cut gasdynamic whistle: 1, moving piston with a pressure gauge; 2, housing; 3, strut; 4, water in/outlets; 5, pressure-gauge cable; and 6, resonant cavity.

Oblique-Cut Gasdynamic Whistle

The evolution of natural and artificial disturbances in a laminar near wake is studied in the wake of an oblique cylindrical whistle. The whistle in the present experiments is used both as a passive body immersed in a hypersonic flow and as a source of artificial disturbances in the wake. A schematic diagram and photo of the whistle on the strut are shown in Fig. 2. The whistle is a 0.07-m-long copper tube, whose outer diameter is $d_w = 8$ mm and inner diameter is 6 mm. The leading end of the tube is obliquely cut at an angle of 20 deg to the tube axis. The trailing end of the tube is closed with a moving piston that is equipped with a piezoelectric pressure gauge. The gauge signal is used to determine the frequency and intensity of pressure pulsations inside the whistle; it is additionally

used as a reference signal when weak periodic signals are detected using the electron-beam-induced fluorescence method. The whistle tube is water-cooled; this cooling maintained the temperature factor of the cone surface at a level of 0.23. The whistle is mounted on a wedge-shaped strut, with a base thickness of 5 mm and a wedge angle of 10 deg.

The whistle, when immersed in a hypersonic flow with its axis parallel to the stream direction, produces intense pressure pulsations. The pulsations, generated in the whistle cavity, are accompanied by a periodic ejection of gas into the shock layer on the whistle and by an associated oscillatory displacement of the shock-wave front's position relative to the whistle nose. The induced disturbances propagate into the wake behind the whistle. By displacing the piston in the tube, the frequency of the pressure pulsations can easily be changed in the range from 1 to 10 kHz. The level of pressure pulsations in the whistle cavity depends on the depth of the resonator cavity, which in turn is directly related to the frequency of the pulsations. In the low-frequency part of the spectrum, the amplitude of the pressure pulsations approaches the pressure behind the normal shock. The frequency spectrum of the pulsations displays narrow peaks at the fundamental frequency of the quarter-wave resonator and also at several of its most intense harmonics. With increasing frequency, the amplitude of the pressure pulsations decreases, and the whole spectrum degenerates into the single peak of the fundamental mode, with its width at half amplitude being 10% of the fundamental frequency. According to previous studies, for all flow modes around the whistle there exists a linear relation between the intensity of pressure pulsations in the whistle cavity and the amplitude of density pulsations in the outside flow around the whistle.

The excitation mechanism of pressure pulsations in the whistle cavity and the relation between the pressure and density pulsations are described in Ref. 25. Previously, a similar oblique gas-dynamic whistle was used to introduce disturbances into a shock flow over a plate.[26]

When performing experiments aimed at revealing the downstream evolution of natural disturbances in the wake behind the whistle, we use a metallic insert that is placed in the whistle cavity. The insert occupies the whistle cavity, thus preventing the generation of pressure pulsations, but keeping the aerodynamic shape of the whistle.

Measurement Technique

To gain data on the characteristics of disturbances in the hypersonic shock layer, we developed a diagnostic technique based on monitoring electron-beam-induced fluorescence of nitrogen.[24] The technique employs the relation between the local gas density and the fluorescence intensity of nitrogen molecules, which are excited by collisions with fast electrons. In the present work this technique was extended to the case of rather dense flows in which the effects upon the fluorescence due to the scattering of the diagnostic electron beam and the quenching action of the excited molecules cannot be ignored. The technique has several attributes; it enables both single-point and two-point measurements of density pulsations; it yields spatial distributions of spectra and phase velocities along the longitudinal and transverse coordinates; and it permits calculation of increments in the disturbance amplitude.

The diagnostic electron beam is generated by a triode electron gun with an indirectly heated cathode. The electron energy is $\cong$12 keV, the electron current is 1 mA, and the diameter of the electron beam in vacuum is about 1 mm. With a magnetic system, we are able to scan the flow with the electron beam in the direction normal to the stream axis (Y coordinate). Scanning along the longitudinal coordinate X is carried out by displacing the model along the stream axis. The axis of the optical system that measures the fluorescence is always normal to the electron beam axis, and the system can be displaced along the beam, that is, along the coordinate Z. The measurement geometry, as exemplified by experiments on revealing the flow structure in the wake behind a cone, is illustrated in Fig. 3.

The mean density fields are reconstructed on the assumption that the major process causing the nonlinear dependence of fluorescence intensity on density is the collision-induced deactivation of molecules. Electron scattering is assumed to be an effect of minor importance because the path of fast electrons in the pressurized gas is rather short. The correction to the mean density for electron scattering is applied in an iterative manner, using the model of exponential attenuation of the electron beam in the gas.[27]

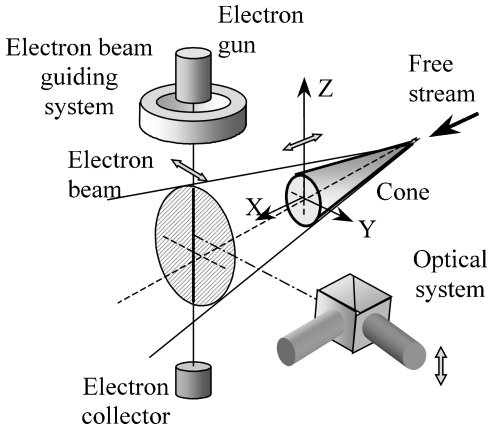

Fig. 3 Measurement scheme used in the experiments.

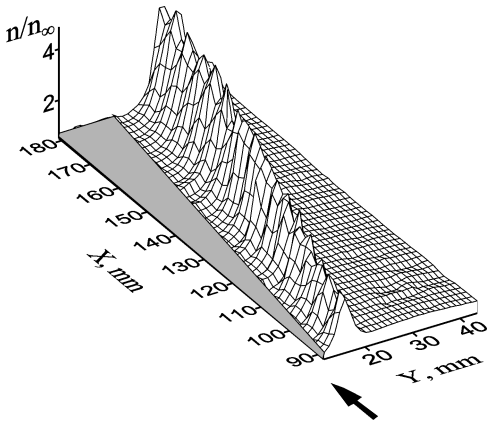

Fig. 4 Distribution of mean density in the shock layer on the 7-deg sharp cone.

The first-order estimate of the mean density is obtained within the framework of the Stern–Volmer model of fluorescence quenching by binary intermolecular collisions.[28–30] The gas temperature behind the compression shock is calculated from shock-adiabatic relations for the shock-wave angle found in experiments using electron beam visualization of the flow. The flow region behind the shock wave shows the highest gas density in the shock layer; in this region, the deactivation process plays a predominant role. The quenching constant is estimated from the experimental data[31] and the gas temperature. The deactivation constant found in this manner is used to calculate the mean gas density in the shock layer. Afterward, a correction to the density for electron scattering is applied in an iterative manner, with two iteration steps being found to be quite sufficient for the process to converge. The absolute value of the correction is no greater than 10% and 15–20% in the high-density region and in the near-surface layer with relatively low gas density, respectively.

With a known mean density field, we can correct the spectral amplitudes of density pulsations for the effect of collisional excitation deactivation according to the procedure described in Refs. 24 and 27. No correction to the spectral amplitude of density pulsations for electron scattering is made, because this effect is already taken into account in reconstructing the mean density, and its influence on the amplitude of the pulsations is a second-order phenomenon.

Evolution of Natural Disturbances in the Shock Layer on a Sharp Cone

Figure 4 shows the field of mean density in the X, Y plane in the shock layer of the 7-deg sharp cone. In the vicinity of the cone vertex,

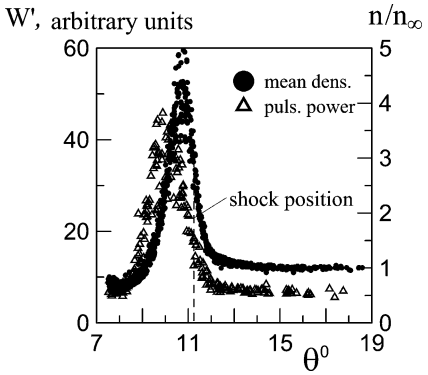

Fig. 5 Distributions of normalized mean density n/n_∞ and power of total density pulsations w' in the shock layer on the 7-deg cone over the angle θ of the conical coordinate system (X, θ). Data are shown for all sections over the coordinate X.

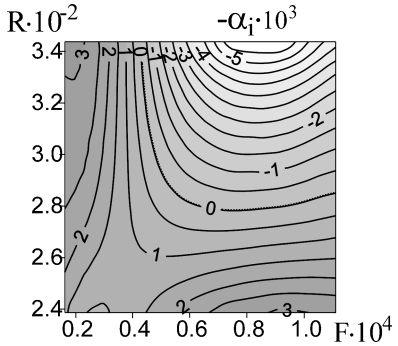

Fig. 6 Distribution of the increment $-\alpha_i$ of natural perturbations in the shock layer of the 7-deg cone in the plane (R, F).

the field is seen to display a typical pattern of conical flow; further downstream, the gas density increases somewhat as we move from the nose. The latter increases can be attributed to the effect due to rarefaction, which diminishes the density jump as compared to the jump in a continuum medium with a low local Reynolds number.[18]

Figure 5 shows the distributions of mean density and energy of total density pulsations over the angle θ for all cross sections over the coordinate X. The angle θ is determined from the cone axis (X direction), and the vertex of the angle coincides with the nose of the cone. The dependencies can be generalized well in the conical coordinate system (X, θ) and a predominant fraction of the pulsation energy is concentrated in a narrow layer underlying the shock wave; the position of this layer is about 0.8 of the shock-layer thickness. The latter finding agrees well with the data obtained for natural density pulsations in the shock layer on a plate.

The spectrum of the increments $-\alpha_i(F)$ of perturbations is shown in Fig. 6 for the points in the corridor of width ±5% of the shock-layer thickness, around the line where the total density pulsations are most intense. Before the calculation of the increments, the logarithmic plot of the density pulsation amplitude vs the R at each frequency F is fitted with cubic splines. Figure 6 shows isolines of the increments $-\alpha_i$ in the plane (F, R). The local Reynolds number is calculated from freestream parameters. It is seen from the graph that the intensity of density pulsations increases most rapidly at low R in the high-frequency band of the spectrum and at high R in its low-frequency band.

Evolution of Disturbances in Hypersonic Laminar Near Wake

Evolution of Natural Disturbances in the Wake Behind the Cone and Whistle

Figure 7 shows the distributions of mean density in the wake behind the sharp nose cone (Fig. 7a) and in the wake behind the gasdynamic whistle in the absence of pressure pulsations in the resonator cavity (Fig. 7b). Here, almost conical flows are observed. The mean-density data for the wake behind the whistle can be generalized well in the conical coordinate system (X, θ), whereas the compression shock line in the wake behind the cone, as revealed by visualization tests, turns out to be somewhat bent toward the wake. The latter effect is most probably related to the rarefaction waves that arise in the diverging flow past the corner at the base of the cone and impinge onto the compression shock.

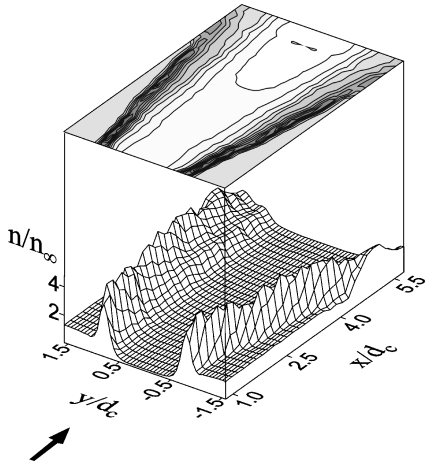

Fig. 7a Field of mean density in the near-wake behind the 10-deg sharp cone.

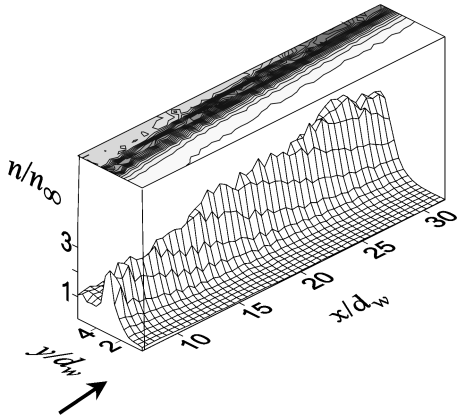

Fig. 7b Distribution of mean density in the wake behind the oblique-cut gasdynamic whistle.

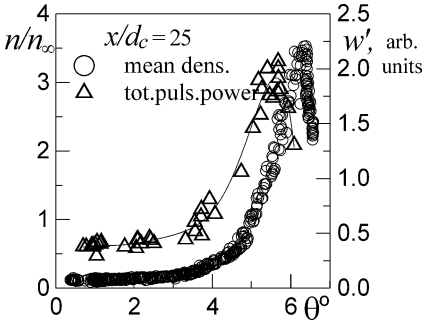

Fig. 8 Distribution of normalized mean density n/n_∞ and power of total density pulsations w' in the wake behind the oblique-cut gasdynamic whistle in the cross section $x/d_w = 25$.

Measurements of mean density and energy of total natural density pulsations in the wakes behind the cone and whistle show that the predominant fraction of the pulsating energy is concentrated in a narrow layer adjacent to the compression shock. [See, for instance, the data obtained from the wake behind the whistle (Fig. 8).] The latter observation qualitatively agrees with the distributions of the energy of total pulsations in a viscous shock layer on a plate[24] or cone.

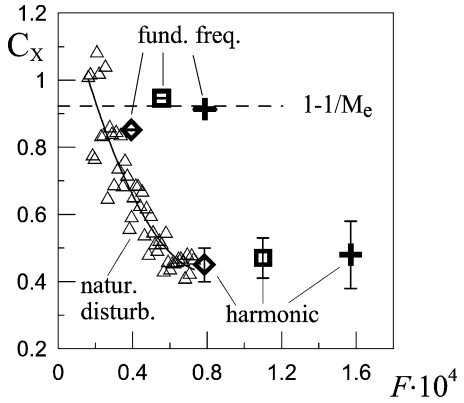

Fig. 9 Spectrum of normalized longitudinal phase velocity C_x of natural density disturbances in the near-wake behind the 10-deg sharp cone and artificial density perturbations in the wake behind the whistle.

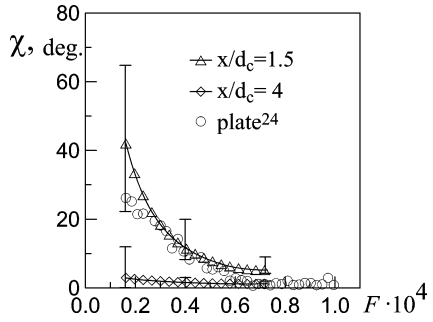

Fig. 10 Spectra of inclination angles of density waves χ in the wake behind the 10-deg sharp cone at two different distances from the cone base. For comparison, data for the flat plate[24] are shown.

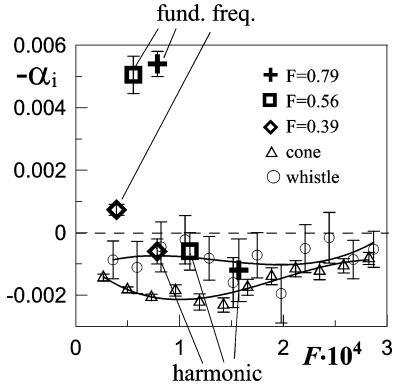

Fig. 11 Spectra of the increments of natural (▲, ○) and artificial density perturbations in the near wakes behind the cone and whistle.

Figure 9 shows the measured spectrum of the normalized longitudinal phase velocity C_x of natural perturbations in the wakes behind the cone and gasdynamic whistle in the absence of pulsations in the whistle cavity. The general shape of the spectrum qualitatively agrees with the data obtained for a plate.[24] In the wake behind the cone, the spectrum of the azimuthal phase velocity, C_ϕ, is also measured. The fraction of inclined waves in the wake near the cone base appears to be rather high; further downstream, this fraction rapidly decreases with distance from the cone base (Fig. 10). The value of the wave inclination angle is found to be substantially lower than that in the freestream (Fig. 1). Most probably, on the cone and in the wake, some relaxation of the spectrum of natural perturbations takes place, during which two-dimensional perturbations predominantly survive. Previous studies[5] have also revealed the presence of inclined waves in the low-frequency portion of the spectrum in the case of a shock layer on a plate.

Figure 11 shows the measured spectra of the increments $\alpha_i(F)$ of natural perturbations in the wakes behind the cone and whistle. The spectrum for the wake behind the cone is obtained from measurements made in the flow region where the density pulsations are most intense, $x/d_c = 1.5$ to 4.0. (The coordinate x here is measured from the cone base.) The spectrum in the wake behind the whistle is obtained from measurements made in the flow region $x/d_w = 8$ to 31. It is seen from the graphs that, in both cases, all natural perturbations decay in the wakes. The more rapid attenuation of pulsations in the wake behind the cone can be explained by the stabilization of initial perturbations under conditions of flow acceleration in rarefaction waves (expectedly, such waves can be less pronounced in the wake behind the narrower body of the whistle).

Evolution of Artificial Disturbances in the Wake Behind the Gasdynamic Whistle

Introduction of artificial disturbances into the wake behind the gasdynamic whistle does not change, the radial distribution of mean density, within the measurement accuracy, but causes instability of the hypersonic wake and growth of flow perturbations at the fundamental frequency (Fig. 12). The intensity of density pulsations at the beginning of the region from which the data are obtained is about 1% of the freestream density. It is seen from the figure that the transverse distributions of density pulsations show two maxima at the inner and outer slopes of the mean-density distribution. The phases of the pulsations at the maxima differ from each other by 180 deg and increase in the downstream direction (Fig. 13). This observation is indicative of wavy radial motion of the wake flow. Figure 9 shows the normalized phase velocities C_x of artificial disturbances at the fundamental frequency and at the harmonic frequency. It is seen that, at the fundamental frequency, the velocities C_x lie close to the separation line between the vertex and acoustic modes, whereas the velocities at the harmonic frequency turn out to be appreciably lower. Figure 10 shows the increments $-\alpha_i(F)$ of artificial disturbances at the fundamental frequency and at the harmonic frequency.

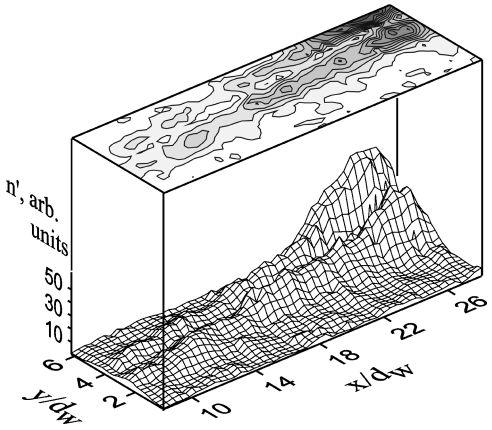

Fig. 12 Distribution of the amplitude of density pulsations in the wake behind the whistle at the fundamental frequency $F = 0.79$ in the (X, Y) plane.

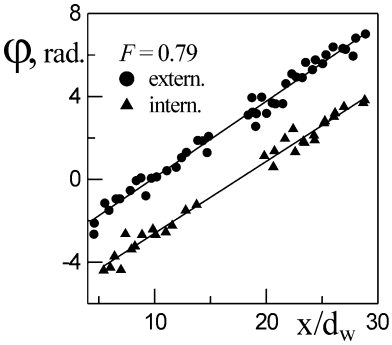

Fig. 13 Phase of artificial disturbances φ in the wake behind the whistle at the fundamental frequency ($F = 0.79$) vs the longitudinal coordinate X.

It is seen from the figure that the disturbances at the fundamental frequency with phase velocities that are close to the separation line between the first and second instability modes grow rapidly in amplitude. Disturbances that are more distant from this line (for instance, those at a frequency of $F = 0.56$) grow more slowly, and the disturbances with low phase velocities at the fundamental frequency decay in a manner that is similar to natural perturbations.

Conclusions

Measurements performed on a 7-deg sharp cone and in the laminar near wake reveal qualitative similarity between the characteristics of natural density perturbations developing in the shock layers of cones, plates, and in their wakes, including 1) predominant concentration of the energy of perturbations in a narrow layer behind the shock wave and 2) occurrence of inclined and two-dimensional density waves in the spectra of pulsations.

In the wake behind the 10-deg sharp cone with natural disturbances, the inclined waves are shown to decay, and the relative fraction of two-dimensional perturbations increases as the general level of perturbations gradually decreases throughout the spectrum.

Introduction of artificial finite-amplitude disturbances into the wake flow results in a loss of its stability. It is shown that the disturbances whose longitudinal phase velocities lie close to the region where the first and second instability modes coexist rapidly grow in intensity, whereas the disturbances with low longitudinal phase velocities decay in very much the same manner as natural perturbations do.

Acknowledgments

This work was supported by the Russian Foundation for Basic Research (Grants 01-01-00189, 02-01-00141, 04-01-00474, and 05-01-00349) and by the International Association for the Promotion of Cooperation with Scientists from the New Independent States of the Former Soviet Union (Grant 2000-0007).

References

[1]Balsa, T. F., and Goldstein, M. E., "On the Instabilities of Supersonic Mixing Layers: A High Mach Numbers Asymptotic Theory," *Journal of Fluid Mechanics*, Vol. 214, 1990, pp. 585–611.

[2]Smith, F. T., and Brown, S. N., "The Linear Inviscid Instability of a Blasius Boundary Layer at Large Values of the Mach Number," *Journal of Fluid Mechanics*, Vol. 219, 1990, pp. 499–518.

[3]Jackson, T. L., and Grosh, C. E., "Inviscid Spatial Stability of a Compressible Mixing Layer," *Journal of Fluid Mechanics*, Vol. 208, 1989, pp. 609–637.

[4]Papageorgiou, D. T., "The Stability of Two-Dimensional Wakes and Shear Layers at High Mach Numbers," *Physics of Fluids A*, Vol. 3, No. 5, 1991, pp. 793–802.

[5]Blackaby, N. D., Cowley, S. J., and Hall, Ph., "On the Instability of Hypersonic Flow past a Flat Plate," *Journal of Fluid Mechanics*, Vol. 247, 1993, pp. 369–416.

[6]Chang, C. L., Malik, M. R., and Hussaini, M. Y., "Effects of Shock on the Stability of Hypersonic Boundary Layers," AIAA Paper 90-1448, June 1990.

[7]Gushin, V. P., and Fedorov, A. V., "Asymptotic Structure of Inviscid Perturbations in a Thin Shock Layer," *Izvestia Akademii Nauk SSSR, Mekhanika Zhidkosti i Gaza*, Vol. 23, No. 6, 1988, pp. 72–79 (in Russian).

[8]Petrov, G. V., "Stability of Thin Viscous Shock Layer on Wadge in Hypersonic Flow of a Perfect Gas," *Laminar-Turbulent Transition. Proceedings of 2nd IUTAM Symposium, Novosibirsk, 1984*, edited by V. Kozlov, Springer-Verlag, Berlin, 1985, pp. 487–493.

[9]Fisher, M. C., Maddalon, D. V., Weinstein, L. M., and Wagner, R. D., Jr., "Boundary-Layer Pitot and Hot-Wire Surveys at $M_\infty \cong 20$," *AIAA Journal*, Vol. 9, No. 5, 1971, pp. 826–834.

[10]Kemp, J. H., and Owen, F. K., "Nozzle Wall Boundary Layer at Mach Numbers 20 to 47," *AIAA Journal*, Vol. 10, No. 7, 1972, pp. 872–879.

[11]Smith, J. A., and Driscoll, J. F., "The Electron-Beam Fluorescence Technique for Measurements in Hypersonic Turbulent Flows," *Journal of Fluid Mechanics*, Vol. 72, No. 4, 1975, pp. 695–719.

[12]Wallace, J. E., "Hypersonic Turbulent Boundary Layer Measurements Using an Electron-Beam," *AIAA Journal*, Vol. 7, No. 4, 1969, pp. 757–759.

[13]Beckwith, I. E., Harvey, W. D., and Clark, F. L., "Comparison of Turbulent Boundary Layer Measurements at Mach Number 19.5 with Theory and an Assessment of Probe Errors," NASA TN-D 6192, 1971.

[14]Lisenko, V. I., "High-Speed Boundary-Layer Stability and Transition," *Engineering Transactions*, Vol. 41, No. 1, 1993, pp. 31–45.

[15]Spina, E. F., and McGinley, C. B., "Constant-Temperature Anemometry in Hypersonic Flow: Critical Issues and Sample Results," *Experiments in Fluids*, Vol. 17, No. 6, 1994, pp. 365–378.

[16]Waldron, H. F., "Viscous Hypersonic Flow over Pointed Cones at Low Reynolds Numbers," *AIAA Journal*, Vol. 5, No. 2, 1967, pp. 208–218.

[17]Harbour, P. J., and Lewis, J. H., "Preliminary Measurements of the Hypersonic Rarefied Flow Field on a Sharp Plate Using Electron Beam Probe," *Rarefied Gas Dynamics*, Suppl. 2, edited by C. L. Brundin, Academic Press, New York, 1967, pp. 1031–1046.

[18]McCroskey, W. J., Bogdonoff, S. M., and Genchi, A. P., "Leading Edge Flow Studies of Sharp Bodies in Rarefied Hypersonic Flow," *Rarefied Gas Dynamics*, Suppl. 2, edited by C. L. Brundin, Academic Press, New York, 1967, pp. 1047–1066.

[19]Vas, I. E., and Sierchio, J. G., "Downstream Effects of Bluntness in the Merged Flow Region," *Rarefied Gas Dynamics*, edited by K. Karamchetti, Academic Press, New York, 1974, pp. 307–315.

[20]Nagamatsu, H. T., and Sheer, R. E., Jr., "Boundary-Layer Transition on a 10° Cone in Hypersonic Flow," *AIAA Journal*, Vol. 3, No. 11, 1965, pp. 2054–2061.

[21]Pallone, A., Erdos, J., and Eckerman, J., "Hypersonic Laminar Wakes and Transition Studies," *AIAA Journal*, Vol. 2, No. 5, 1964, pp. 855–863.

[22]Livensteins, Z. J., and Krumins, M. V., "Aerodynamic Characteristics of Hypersonic Wakes," *AIAA Journal*, Vol. 5, No. 9, 1967, pp. 1596–1602.

[23]Lykoudis, P. S., "A Review of Hypersonic Wake Studies," *AIAA Journal*, Vol. 4, No. 4, 1966, pp. 577–590.

[24]Mironov, S. G., and Maslov, A. A., "An Experimental Study of Density Waves in a Hypersonic Shock Layer on a Flat Plate," *Physics of Fluids A*, Vol. 12, No. 6, 2000, pp. 1544–1553.

[25]Maslov, A. A., and Mironov, S. G., "Experimental Investigation of the Hypersonic Low-Density Flow past a Half-Closed Cylindrical Cavity," *Fluid Dynamics*, Vol. 31, No. 6, 1996, pp. 928–932.

[26]Mironov, S. G., and Maslov, A. A., "Experimental Study of Secondary Instability in a Hypersonic Shock Layer on a Flat Plate," *Journal of Fluid Mechanics*, Vol. 412, 2000, pp. 259–277.

[27]Aniskin, V. M., and Mironov, S. G., "Experimental Study of Density Pulsations in Hypersonic Laminar Wake Behind a Cone," *Journal of Applied Mechanics and Technical Physics*, Vol. 41, No. 3, 2000, pp. 395–402.

[28]Muntz, E. P., and Softley, E. J., "A Study of Laminar Near Wakes," *AIAA Journal*, Vol. 4, No. 6, 1966, pp. 961–968.

[29]Tardif, L., and Dionne, J. G. G., "Density Distribution in Turbulent and Laminar Wakes," *AIAA Journal*, Vol. 6, No. 10, 1968, pp. 2027–2029.

[30]Dionne, J. G. G., and Tardif, L., "Density and Temperature Distributions in Hypersonic Sphere Wakes," *Canadian Journal of Physics*, Vol. 51, No. 8, 1973, pp. 852–860.

[31]Belikov, A. E., Kusnetsov, O. V., and Sharafutdinov, R. G., "The Rate of Collisional Quenching of N_2O^{*+}, N_2^{*+}, O_2^{*+}, O^{*+}, O*, Ar*, Ar^{*+} at the Temperature < 200 K," *Journal of Chemical Physics*, Vol. 102, No. 5, 1995, pp. 2792–2798.

T. Lin
Associate Editor